

S. KÜHN
V. SANDOGHDAR 

Modification of single molecule fluorescence by a scanning probe

Laboratorium für Physikalische Chemie, ETH Zürich, 8093 Zürich, Switzerland

Received: 10 January 2006**Published online: 13 May 2006 • © Springer-Verlag 2006**

ABSTRACT We examine the optical near-field interaction between different types of scanning tips and single oriented fluorescent molecules. We demonstrate the influence of a tip on the excitation intensity as well as on the integrated fluorescence signal, the excited state lifetime, and the angular emission of single molecules. By using a standard model describing the radiation of an oscillating dipole close to a nanosphere or a flat interface, we interpret our observations and describe some central criteria for obtaining fluorescence enhancement or quenching.

PACS 33.80.-b; 07.79.Fc; 78.90.+t

1 Introduction


Rough surfaces are known to change the absorption, scattering and emission cross sections of molecules placed in their close proximities [1]. The most celebrated effect in this context is surface enhanced Raman scattering (SERS). However, fluorescence has also been reported to experience a substantial increase close to metallic rough surfaces. This is particularly intriguing because one typically expects the fluorescence to be quenched for emitters located very close to real metals [2]. For this reason, and because fluorescence can be detected with a very high signal-to-noise ratio, several recent experiments have chosen to investigate the modification of fluorescence from single emitters close to nanostructures [3–9]. An especially powerful technique for such studies has been the use of scanning probe methodology due to its potential to control the position and orientation of a well-defined nanostructure with respect to a well characterized single emitter. The most commonly used “nanostructures” in this approach, however, have been extended, uncoated [5–7], or metallized AFM tips [4]. In some of these cases enhancement [6, 7], whereas in others quenching [4], of fluorescence has been reported.

The excitation process is expected to be modified by the enhancement of the illumination field at sharp edges (also known as the lightning rod effect), due to surface plasmons, or due to resonant antenna effects. Furthermore, modification

of the spontaneous emission and the nonradiative decay rates close to the tip are expected to alter the emission process. Deciphering these phenomena, however, poses a great experimental challenge because they are not only often present simultaneously, but each also depends strongly on the separation and orientation between the molecule and the nanostructure. We have recently reported on a near twenty-fold enhancement of fluorescence and a twenty-fold reduction of the excited state lifetime in the near field of a gold nanoparticle attached to a tip [9]. In that work we demonstrated the role of resonant enhancements of the excitation via particle plasmons, and discussed the competition between quenching and the enhancement of spontaneous emission at the plasmon resonance. Here we consider two types of probes: a glass tip to eliminate quenching and chromium-coated glass tips to avoid plasmon resonances. By using a classical model that takes into account the interaction of a dipole close to a spherical particle [10], we provide some criteria for obtaining enhancement versus quenching. Furthermore, we investigate the influence of the tip on the distribution of the excitation field and on the angular emission spectrum of the molecule.

2 Experimental

Aside from the results presented in Fig. 6, all data were obtained using samples produced by spin coating a solution of terrylene (10^{-7} M) and para-terphenyl (pT, 3 mg/ml) in toluole onto a cleaned glass microscope cover slide. We have shown that such samples consist of very thin pT films [11] where terrylene molecules lie at a slight angle of about 15° from the normal to the substrate [12]. Furthermore, our previous work shows that terrylene molecules in this matrix maintain a near to one quantum efficiency, and possess an unprecedented photostability and show almost no blinking intermittency. These features make this system an excellent candidate for near-field fluorescence studies at the single molecule level [9, 12]. To visualize single terrylene molecules, wide-field fluorescence images were taken on an inverted microscope using total internal reflection excitation with *p*-polarized light at a wavelength of 532 nm. This was achieved by focussing the excitation laser beam at the entrance aperture plane of the microscope objective (Zeiss, 1.4 NA) offset from its axis, to produce an angle of incidence of 40° in the pT film ($n_{\text{pT}} \sim 1.85$). In this excitation

 Fax: +41-44-633-1316, E-mail: vahid.sandoghdar@ethz.ch

mode a relatively large area of $10 \times 10 \mu\text{m}^2$ is illuminated. At higher magnification ($260\times$) the molecules appear as well-separated doughnut-like shapes on a CCD camera. Alternatively, the fluorescence from an isolated molecule could be detected through a pinhole using an avalanche photodiode (APD). We have verified that in all our measurements the fluorescence signal scales linearly with the excitation intensity; i.e. we operate far from saturation.

To study the influence of a local probe on the molecular fluorescence, we used the machinery of a home-built scanning near-field optical microscope (SNOM) housed on the inverted microscope to manipulate the probe in the immediate vicinity of the sample surface. The separation between the tip and the sample could be either locked at about 5 nm using shear force feedback control (constant gap mode) or be set to arbitrary values, using a piezo actuator (variable gap mode). In either case images were acquired by scanning the tip laterally and recording a signal from a single molecule. The results discussed in this work were all obtained using heat pulled tips produced by a Sutter P-2000 micropipette puller. Such tips can be produced to be sharp with a radius of curvature as small as about 40 nm. However, depending on the parameter settings, the tip could also have a flat end with a diameter of a few hundred nanometers. This plateau is sometimes accompanied by a sharp protrusion.

Figure 1a shows a near-field fluorescence image recorded when scanning an uncoated glass tip in the constant gap mode. Figure 1b displays the topography map of the sample taken simultaneously, measuring a sample height of about 45 nm. Figure 1c shows another scan with a higher pixel resolution of the central region marked in Fig. 1a, where the location of the molecule is labelled by an arrow. Figure 1d illustrates a cross section from Fig. 1a. These data clearly reveal an increase of molecular emission by about 60% when the glass tip is right above the molecule. In addition to this local enhancement of

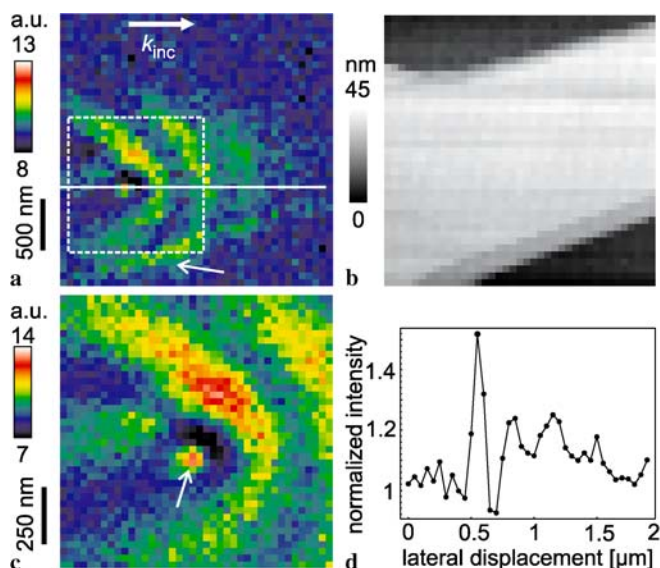


FIGURE 1 (a) Fluorescence of a single molecule when a sharp glass tip is scanned above the sample. (b) Topography image recorded simultaneously as in (a). (c) A second high pixel resolution scan of the region marked by the white square in (a). The arrow signifies the location of the molecule. (d) Cross-section along the line indicated in (a)

the fluorescence, we identify a modulation of emission caused by the interference between the incident beam (direction indicated by the vector k_{inc}) and the light scattered by the tip [6, 13, 14]. When the tip is before the molecule (to the left of the molecule) the incident beam and its scattered component co-propagate, resulting in a uniform intensity. But as the tip moves beyond the molecule the field scattered by the tip counter-propagates against the incident laser beam, forming a standing wave pattern that modulates the excitation intensity at the position of the molecule. These features are well recovered in numerical calculations [13] and have been recently verified both by near-field lithography [14] and by single molecule fluorescence measurements [6]. However, in Fig. 1a and c we also observe a clear asymmetry signified by a stronger signal toward the upper right side. This is caused by the slight tilt of the molecular dipole (by about 15°) that results in a better match with the back-scattered field at a particular tip location [6]. Furthermore, in this particular direction the first destructive interference is effective enough to lower the fluorescence signal below that of the isolated molecule. Another noteworthy feature of the signal in Fig. 1a is the truncation of the fluorescence in the lower right side, indicated by an arrow. A comparison with the topography image in Fig. 1b lets us attribute this effect to scattering at the edge of the pT film.

Various theoretical [13, 15–17] and experimental [4, 9, 18–21] reports have shown that the fluorescence lifetime is also modified in the presence of nanostructures. As in the case of an emitter in front of a planar mirror [2], the radiative decay rate can be either reduced or enhanced, depending on the orientation of the molecular dipole. If the dielectric constant of the surrounding medium possesses a nonzero imaginary part, nonradiative decay of the excited state caused by the dissipation of dipolar energy, i.e. quenching, dominates at very small separations. Most laboratory measurements have so far reported the reduction of lifetimes in the presence of tips, and have attributed it to quenching [4, 5, 18, 19]. We examine the effect of a sharp glass tip on a terrylene molecule that is ori-

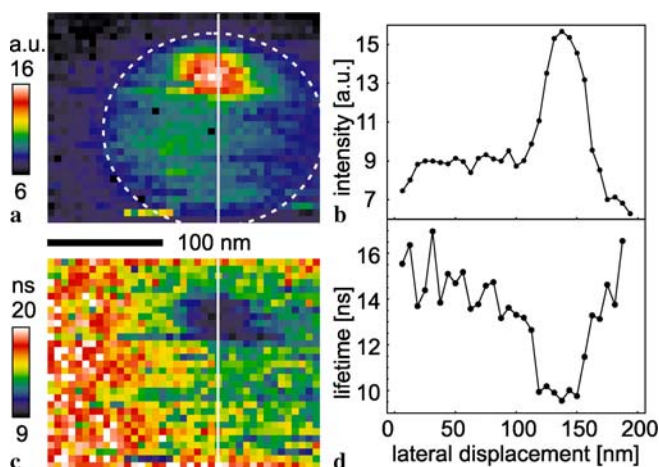


FIGURE 2 (a) Fluorescence near-field image of a single molecule in constant gap mode taken with a glass tip. (c) Map of the lifetime recorded at each pixel of image (a). (b) and (d) show cross-sections along the lines indicated in (a) and (c), respectively. The dashed circle indicates the influence of the plateau at the end of the tip

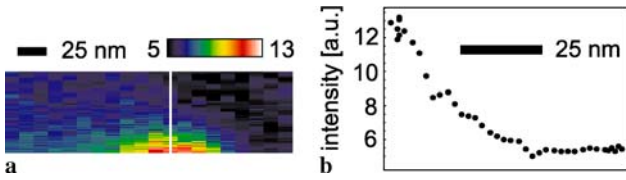


FIGURE 3 (a) Fluorescence image of a molecule in variable-gap mode. At each pixel of a single scan line of Fig. 2 the tip is retracted and re-approached in the vertical direction. (b) Intensity cross-section along the *line* indicated in (a)

ented nearly parallel to the tip axis. The advantage of this system is that quenching is absent because glass has a negligible absorption in the visible domain.

To acquire the fluorescence lifetime, we replaced the continuous wave excitation with a pulsed laser beam and performed time correlated single photon counting by the APD. Measurements of the fluorescence lifetime (18 ns), local film thickness (45 nm) and inclination angle of a single molecule (15°) in the absence of the tip let us deduce that the depth of the molecule below the pT-air interface is 22 nm [12]. Figure 2a and c show a fluorescence image and a map of the excited state lifetime τ taken simultaneously at each tip position, respectively. We find a reduction of the lifetime by about a factor of 2 to $\tau = 9$ ns accompanied by a two-fold increase of the fluorescence signal when the tip is right above the molecule. Cross sections displayed in Fig. 2b and d reveal a sharp lateral confinement in both intensity and lifetime with a full width at half maximum (FWHM) of about 35 nm and a weaker enhancement within about 200 nm indicated by the dashed circle in Fig. 2a. We attribute the tighter confinement to the effect of a sharp protrusion and the broader distribution to a plateau at the end of the tip.

We have also examined the fluorescence signal while moving the tip in a plane normal to the sample and containing the molecule. Figure 3 shows such a vertical map and a cross section from it. The enhancement effect is strongly confined to a short range of about 15 nm. We point out that the decay length of the evanescent excitation beam at an angle of incidence of 40° amounts to about 200 nm, which is considerably longer than the observed decay length. Thus, we conclude that the extreme confinement of the measured effects are due to the tip-induced local increase of the excitation intensity.

To discuss the role of possible mechanisms at play, let us consider the fluorescence intensity S_f in the unsaturated regime, given by

$$S_f \propto \xi I_0 d_{eg}^2 \eta(\mathbf{r}) K(\mathbf{r}). \quad (1)$$

Here ξ denotes an overall detection efficiency, and K accounts for the change of the electric field intensity near the nanostructure as well as its projection onto the direction of the molecular dipole moment. The quantities I_0 and d_{eg} stand for the incident excitation intensity in the absence of the nanostructure, and for the matrix element associated with the transition between the excited and ground states. The vector \mathbf{r} represents the relative displacement between the tip and the emitter. The quantum efficiency η is defined as the ratio $\gamma_r/(\gamma_r + \gamma_{nr})$ where γ_r and γ_{nr} denote the radiative and nonradiative decay rates. In other words, η describes the probability that each decay

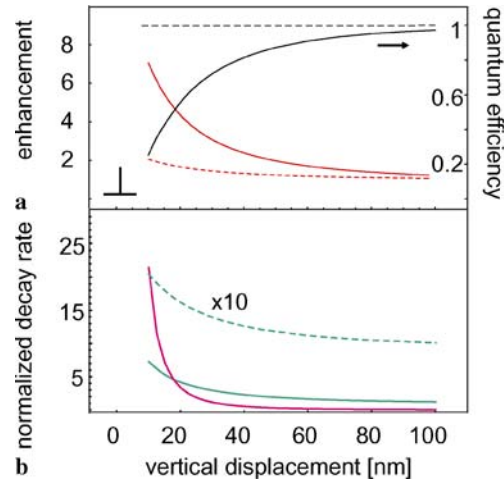


FIGURE 4 Calculations for an oscillating dipole emitting at a wavelength of 580 nm, placed close to dielectric (*dashed curves*) and chromium (*solid lines*) spheres of diameter 100 nm, and oriented radially. (a) *Red curves* show excitation enhancement of a plane wave illumination at a wavelength of 532 nm and polarization along the dipole–sphere axis. *Black curves* display the quantum efficiency. (b) The *green and the pink curves* show the radiative and nonradiative decay rates respectively, normalized to the decay rate of the unperturbed dipole

of the excited state results in the emission of a photon. Since the near unity quantum efficiency of a terrylene molecule [12] cannot be changed by the presence of a glass tip, enhancement of S_f can only be due to an increased excitation intensity right below the tip (K) or a more efficient collection of fluorescence (ξ). For a molecule embedded in an ultrathin film with an orientation normal to the substrate, the great majority of the fluorescence enters the substrate and about 70% is already collected by a microscope objective of numerical aperture $NA = 1.4$. Therefore, a slightly higher ξ value in the presence of the tip cannot explain a two-fold enhancement, leaving an increase in K as the only mechanism for the observed enhancement of S_f .

A semiquantitative estimate of the above-mentioned effects can be obtained by approximating the tip with a nanosphere of dielectric constant ϵ and radius R . In this case Mie theory can be used to calculate the field intensity at a given separation from the sphere [22]. The dashed red curve in Fig. 4a displays the normalized electric field intensity in the radial direction close to a glass sphere ($\epsilon = 2.3$) with a diameter of 100 nm. The incident intensity is enhanced by about 60% at a distance of 20 nm from the nanosphere surface and falls to half its value within about 10 nm, in fairly good agreement with the experimental results presented in Figs. 2 and 3. For a sphere of radius R much smaller than the transition wavelength, these results can also be obtained using the quasistatic approximation of the Mie theory where the sphere is substituted by a dipole moment proportional to $R^3 \left(\frac{\epsilon-1}{\epsilon+2}\right)$ [22]. This model shows that 1) the intensity enhancement scales as $\left(\frac{\epsilon-1}{\epsilon+2}\right)^2$ and 2) the field enhancement at the sphere surface is independent of its radius. The latter follows from the fact that the $(1/R)^3$ dependence of the electric field is balanced by the R^3 dependence of the sphere polarizability. These considerations together with the calculated value of 3 for the intensity enhancement at the surface of a glass tip ($\epsilon = 2.3$) let us infer an intensity enhancement of about 20 times at a silicon AFM

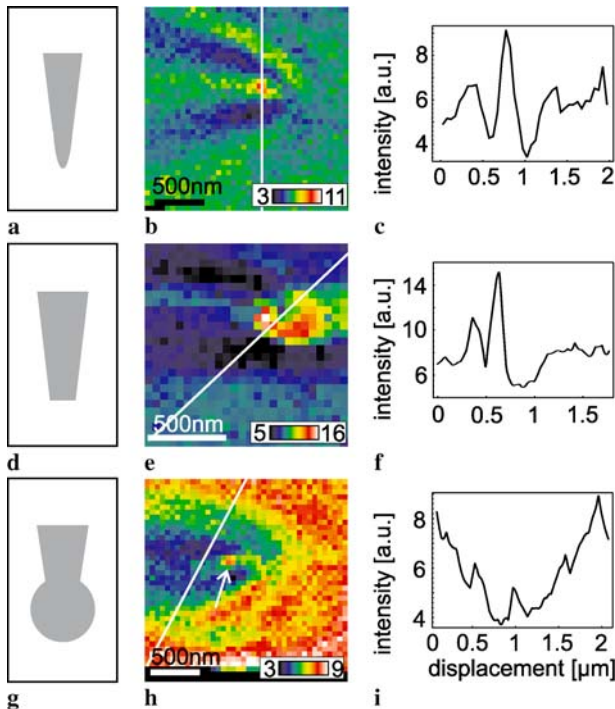


FIGURE 5 Fluorescence scanning probe images of single molecules for three chromium coated tips. (a), (d) and (g) show sketches of the tips in measurements presented in (b), (e), and (h) respectively. (c), (f) and (j) plot cross-sections from fluorescence maps (b), (e) and (h) respectively

tip ($\varepsilon \sim 16$ at a wavelength of 600 nm), in very good agreement with the observations of Gerton et al. [7].

Approximating the tip by a nanosphere also allows analytical solutions for the modification of the fluorescence lifetime following a classical model [10, 23, 24]. The green dashed curve in Fig. 4b displays the distance dependence of the radiative decay rate of a radially oriented dipole close to a glass sphere of diameter 100 nm. We find that at a separation of 20 nm the lifetime is reduced by about 70%, again in good agreement with our measurements. We remark that both our calculations of the field intensity and decay rate modification have been simplified by ignoring the sample–air interface. Although the general trend should persist in full calculations, quantitative agreement with experimental data can only be obtained if the substrate is taken into account properly.

The data presented in Figs. 2 and 3 show that even a dielectric tip could enhance the excitation and emission of an emitter by a moderate factor. We now turn to the metallized tips commonly used in apertureless SNOM [25, 26]. Here we used glass tips coated with 30–40 nm of chromium. Chromium exhibits a strong damping of optical currents due to a large imaginary part of its dielectric function, and it does not support plasmon resonances in the visible spectral range. Figure 5b shows the experimental results performed with a Cr-coated sharp tip (sketched in Fig. 5a) scanned across a terrylene-doped pT sample with a thickness of 20 nm (a different sample than that used in Figs. 1–3). We observe an enhancement of single molecule fluorescence by about 1.6 times within an area of FWHM ~ 150 nm. Moreover, we note an interference pattern in S_f when the tip is placed away from the position of the molecule, similar to that shown in Fig. 1.

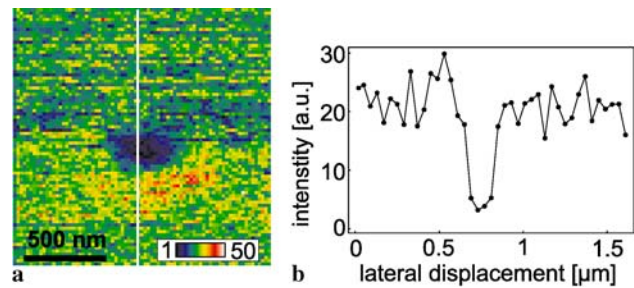


FIGURE 6 Confocal arrangement. (a) Fluorescence scanning probe image of a DiI molecule using a chromium coated glass tip. (b) Cross-section along the line indicated in (a)

Next, we replace the terrylene-pT sample by a polymer (PMMA) thin film of thickness 20–30 nm, containing sparsely dispersed DiI-molecules to study the effect of a sharp metallic tip on a molecule with a dipole moment aligned in the plane of the substrate. Here, we excited single molecules with a linearly polarized focused laser beam propagating along the tip axis (a different but similar tip as used earlier) and obtained images such as that in Fig. 6 when scanning the tip. As opposed to the case of an axially oriented terrylene molecule, we now observe a reduction of the DiI fluorescence to the background level in the presence of the Cr tip. The FWHM of this quenching effect is about 160 nm. We also point out in passing that the interference patterns are absent in Fig. 6 because in this excitation mode the tip is illuminated only when it passes the tight laser focus.

Again, we can obtain a theoretical estimate of the above-mentioned results if we approximate the tip by a small chromium sphere. Considering that the skin depth of Cr for the visible light is as short as 20 nm, and that Cr does not support plasmon resonances in the visible range, we approximate a sharp glass tip covered with 30–40 nm of Cr by a solid

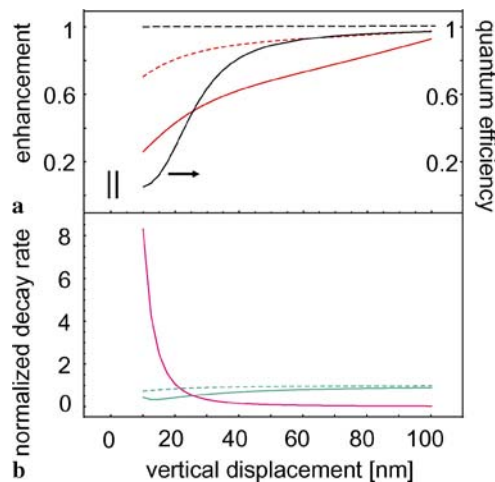


FIGURE 7 Calculations for an oscillating dipole emitting at a wavelength of 580 nm, placed close to dielectric (dashed curves) and chromium (solid lines) spheres of diameter 100 nm, and oriented tangentially with respect to the sphere. a) Red curves show excitation modification of a plane wave illumination at a wavelength of 532 nm and with polarization parallel to the dipole. Black curves display the quantum efficiency. b) The green and the pink curves show the radiative and nonradiative decay rates respectively, normalized to the decay rate of the unperturbed dipole

chromium sphere, using the tabulated bulk dielectric constants of $-8.5 + 29i$ for Cr [27]. We present the intensity enhancement (red curve) and quantum efficiency (black curve) for dipoles oriented in the radial and tangential directions in Figs. 4a and 7a, respectively. In Figs. 4b and 7b we plot the radiative (green) and nonradiative (pink) decay rates for the two dipolar orientations of interest. We see that at a distance of 10 nm from the sphere surface, the excitation intensity is enhanced by about 7 times in the radial direction while it is reduced by about 4 times in the tangential direction. Furthermore, for a radially oriented molecule γ_r and γ_{nr} are enhanced by 7 and 21 times, respectively, reducing η to 25%. For a molecular dipole oriented in the plane of the substrate we find that γ_r is inhibited to 50% of its unperturbed value and γ_{nr} is reduced by 8 times, resulting in $\eta = 5\%$. So, at a separation of about 10 nm, we expect S_f to be increased by about twice for a radially oriented dipole and reduced by about 80 times for a tangentially oriented dipole moment.

Before we continue with the presentation of experimental results, we remark on some aspects of the calculations presented in Fig. 7 for a tangentially oriented dipole. First, the excitation intensity is reduced close to both dielectric (dashed curve) and metallic (solid line) sphere tips. This is caused by the destructive interference between the incident field and the scattered field of the sphere. Again, the essential feature can be best visualized by replacing the sphere with an induced dipole at its center. It is then readily seen that the field at a location perpendicular to the dipole's axis is antiparallel to the induced dipole moment and the incident field. Therefore, the total excitation field is lowered. Another noteworthy effect is that the radiative decay, i.e. spontaneous emission, is slowed down for this dipolar orientation. In case of a dielectric tip, there is no quenching, and the quantum efficiency remains unchanged (see black dashed lines in Figs. 4 and 7). Therefore, according to (1) one does not expect the emission efficiency to be changed. However, if a large inhibition of spontaneous emission takes place, the overall emission can become so weak that in practice the signal disappears under the background noise. Finally, in light of this discussion, we point out that the reduction of fluorescence under dielectric tips should not be associated with quenching [5] since there is no dissipation of energy involved.

An important parameter that determines the amount of field enhancement and spontaneous emission modification is the shape of the nanostructure [17, 28]. Controlled fabrication

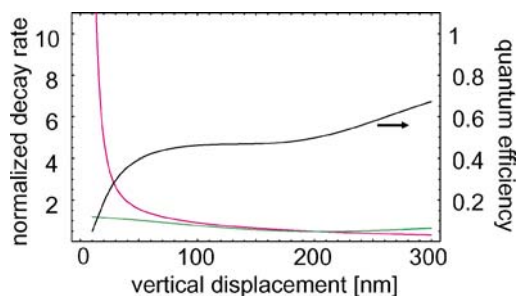


FIGURE 8 Calculated rates for radiative (green) and nonradiative (pink) decay, as well as the resulting quantum efficiency (black) for a dipole approaching a chromium half-space, oriented normal to the interface. The decay rates are normalized to the decay rate of the unperturbed dipole

of tips with various geometry has posed a challenge in SNOM work over nearly twenty years. Nevertheless, we now present two examples of metallized tips that deviate from ideal sharp probes. Figure 5d shows a sketch of a heat pulled tip with a plateau, similar to that applied in Fig. 2, but coated with chromium and without the sharp protrusion. The sample used here was again pT containing oriented terrylene molecules with a typical thickness of 20–30 nm. The illumination is also via total internal reflection so that the molecule is always excited. In Fig. 5, we find that the molecular fluorescence is quenched when the molecule is right below the tip, but it is clearly enhanced on a ring-like set of locations. The enhancement of the fluorescence at the edges of the tip could be attributed to the local field enhancement in a similar fashion as in Fig. 5a where a sharp tip was used. Regarding the reduction of fluorescence in the middle of the tip, we first note that the electrostatic lightning rod type of field enhancement is absent at a locally flat geometry. Next, we consider the radiative and nonradiative rates of a dipole perpendicular to a flat mirror displayed by the green and pink curves in Fig. 8. As expected, we find that a flat surface also causes quenching. In fact, we note that quenching is already significant at a distance of 200 nm for a chromium coated mirror. The longer interaction range displayed in Fig. 8 reflects a general property that near-field effects take effect within a very short distance close to a sharp tip, whereas the influence of blunt tips can be important even at larger distances.

Figure 5h shows further results where a glass fiber tip is slightly molten after fabrication and formed a small sphere with a radius of the order of a few micrometers at the end. The tip was then coated with chromium. The sketch of such a tip is depicted in Fig. 5g. Now we find that the fluorescence signal of a single terrylene molecule drops to the background level (3.5 units on the y-axis of Fig. 5j) for the smallest gap between the tip surface and the molecule. As the tip is laterally scanned away from the molecule, the mirror–molecule separation is increased and the fluorescence is slowly recovered. We observe no enhancement, however, there is a small region with a lateral width of about 100 nm (indicated by an arrow) where the fluorescence signal reaches that of the undisturbed molecule. We have observed such effects in several tips and attribute them to protrusions leading to a small enhancement effect, or indentations resulting in reduced quenching. More details of the modifications of the fluorescence intensity and lifetime of a molecule close to tips with such large radii of curvature were presented in a recent publication [12].

Having discussed tip-induced modification of fluorescence intensity and lifetime, we now present some results on the modification of the emission pattern. This effect has been predicted theoretically [29] and confirmed experimentally [30]. The reported measurements were performed by dividing the collected fluorescence into two channels and monitoring the balance between the two signals as a function of tip location. In our work, we have recorded and analyzed full CCD camera snapshots of the same single molecule emission at high magnification. An undisturbed molecule produces a doughnut-like intensity distribution on the CCD camera as can be seen in Fig. 9a and sketched in Fig. 9 α . This shape is a direct consequence of the nearly axial orientation of the molecular dipole in the sample [11, 12, 31]. Figure 9b–i shows

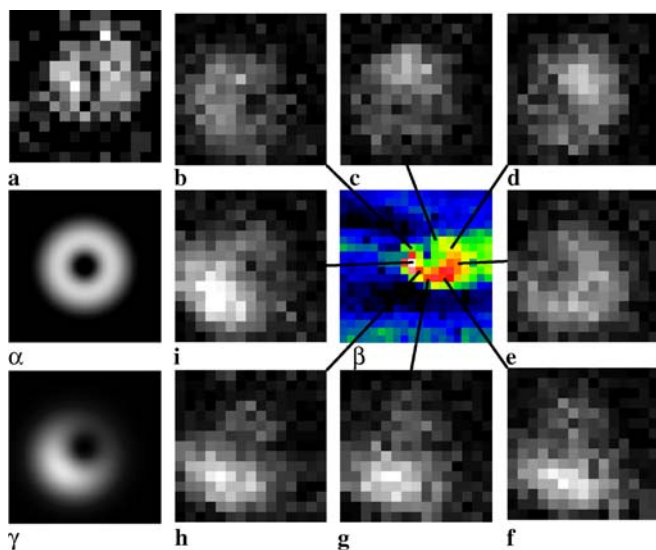


FIGURE 9 Selection of emission patterns of a single terrylene molecule as observed on a CCD camera. (a) A typical doughnut-shaped pattern of an unperturbed molecule. Images (b)–(i) exhibit a selection of disturbed patterns in the presence of the blunt chromium-coated tip. Each image is assigned to the corresponding pixel in (j). (k) and (l) display sketches of the emission pattern for an unperturbed molecule and one influenced by the tip, respectively

a selection of emission patterns recorded at different scan pixels of Fig. 5e. The assignment of each CCD image to the corresponding pixel is indicated by lines linking it to the central part of the original scan displayed again in Fig. 9j. These images show that the weight of the intensity distribution is most strongly modified at the edges of the tip, almost forming a circle on the crest of the intensity image of Fig. 9j. A tentative explanation is given by an analogy to coupled antennae [32]. If we consider the molecule as an oscillating dipole and the tip as a secondary dipole that is driven by the field of the molecule, then the overall system consists of two coherent antennae separated by the vector r . The emission pattern of this elementary antenna-array will deviate from that of a single dipolar antenna and no longer exhibits symmetry around its axis. Figure 9l illustrates a sketch of such a distorted emission pattern. We remark that no notable change in the emission pattern could be detected under the influence of sharp tips (Fig. 5a). In this case, the small spatial extent of a sharp tip and the very short coupling range allows the system to be modelled by two point-like dipoles at a separation much smaller than the wavelength. The emission pattern of such a coupled system is very close to that of a single dipole.

3 Conclusions

We have examined the modification of fluorescence induced by an extended scanning probe and have reported both enhancement and quenching of single molecule fluorescence. Detailed quantitative results on the interaction of a single molecule and a single gold nanoparticle acting as a resonant nanoantenna are published elsewhere [9]. In this work we have chosen our probes to avoid plasmon resonances and concentrated on the quasistatic field enhancement phenomenon, also known as the lightning rod effect. We have re-

ported the enhancement of both the spontaneous emission rate and overall fluorescence signal for a single oriented molecule under a sharp glass tip. We have provided a semiquantitative explanation of these findings using an elementary model of a classical oscillating dipole close to a dielectric sphere. Furthermore, we have demonstrated the modification of fluorescence in the near field of chromium coated glass tips. For a sharp Cr coated probe, we have measured moderate enhancement of fluorescence for molecules oriented parallel to the tip axis and have obtained quenching of the emission for molecules oriented perpendicular to the tip axis. Moreover, we have investigated the effect of less sharp tips that have subwavelength plateaus or micron-sized radii of curvature. These results were also interpreted successfully using the model of a molecule close to a chromium nanosphere. The calculations presented in this work have been approximate, but they have correctly interpreted all the main features of our experimental findings. Our aim was not to achieve a quantitative agreement with the measured data, but rather to point to and describe the coexistence of different processes that compete at the nanometer scale. To this end, the results in Figs. 4, 7 and 8 together with (1) provide the basic criteria for predicting the magnitude and sign of the modification of fluorescence of a molecule at different separations and orientations with respect to a tip. Our investigations provide important criteria for the prediction and interpretation of the contrast mechanism in apertureless SNOM imaging of fluorescence phenomena. We conclude that although apertureless SNOM can readily provide spatial resolution well below 100 nm, when combined with light emitting samples, it can lead to complex images with nontrivial interpretation. Quantitative information on the relative separation and orientation of the molecules with respect to the tip will be crucial for a proper analysis of images.

ACKNOWLEDGEMENTS We thank U. Håkanson for help with the experimental setup and careful reading of the manuscript. This work was supported by the Swiss National Foundation and the Swiss Ministry of Education and Science (EU IP-Molecular Imaging).

REFERENCES

- 1 M. Moskovits, *Rev. Mod. Phys.* **57**, 783 (1985)
- 2 R.R. Chance, A. Prock, R. Silbey, *Adv. Chem. Phys.* **31**, 1 (1978)
- 3 K.T. Shimizu, W.K. Woo, B.R. Fisher, H.J. Eisler, M.G. Bawendi, *Phys. Rev. Lett.* **89**, 117401 (2002)
- 4 W. Tröbsinger, A. Kramer, M. Kreiter, B. Hecht, U. Wild, *Appl. Phys. Lett.* **81**, 2118 (2002)
- 5 W. Tröbsinger, A. Kramer, M. Kreiter, B. Hecht, U. Wild, *J. Microsc.* **209**, 249 (2003)
- 6 V. Protasenko, A. Gallagher, *Nano Lett.* **4**, 1329 (2004)
- 7 J.M. Gerton, L.A. Wade, G.A. Lessard, Z. Ma, S.R. Quake, *Phys. Rev. Lett.* **93**, 180801 (2004)
- 8 J. Farahani, D.W. Pohl, H.-J. Eisler, B. Hecht, *Phys. Rev. Lett.* **95**, 017402 (2005)
- 9 S. Kühn, U. Håkanson, L. Rogobete, V. Sandoghdar, submitted (2005), <http://arxiv.org/abs/cond-mat/0604474>
- 10 P.C. Das, A. Puri, *Phys. Rev. B* **65**, 155416 (2002)
- 11 R.J. Pfab, J. Zimmermann, C. Hettich, I. Gerhardt, A. Renn, V. Sandoghdar, *Chem. Phys. Lett.* **387**, 490 (2004)
- 12 B.C. Buchler, T. Kalkbrenner, C. Hettich, V. Sandoghdar, *Phys. Rev. Lett.* **95**, 063003 (2005)
- 13 C. Girard, O.J.F. Martin, A. Dereux, *Phys. Rev. Lett.* **75**, 3098 (1995)
- 14 F. H'Dhili, R. Bachelot, A. Rumyantseva, G. Lerondel, P. Royer, *J. Microsc.* **209**, 214 (2003)

- 15 H. Metiu, *Prog. Surf. Sci.* **17**, 153 (1984)
- 16 C. Henkel, V. Sandoghdar, *Opt. Commun.* **158**, 250 (1998)
- 17 L. Rogobete, H. Schniepp, V. Sandoghdar, C. Henkel, *Opt. Lett.* **28**, 1736 (2003)
- 18 W.P. Ambrose, P.M. Goodwin, J.C. Martin, R.A. Keller, *Science* **265**, 364 (1994)
- 19 X.S. Xie, R.C. Dunn, *Science* **265**, 361 (1994)
- 20 J.D. Pedarnig, M. Specht, T.W. Hänsch, in *Photons and Local Probes*, ed. by O. Marti, R. Möller (Springer, Berlin, 1995), p. 151–163
- 21 H. Schniepp, V. Sandoghdar, *Phys. Rev. Lett.* **89**, 257403 (2002)
- 22 C.F. Bohren, D.R. Huffman, *Absorption and Scattering of Light by Small Particles* (Wiley, New York, 1983)
- 23 R. Ruppin, *J. Chem. Phys.* **76**, 1681 (1982)
- 24 H. Chew, *J. Chem. Phys.* **87**, 1355 (1987)
- 25 F. Zenhausern, M. P. O'Boyle, H.K. Wickramasinghe, *Appl. Phys. Lett.* **65**, 1623 (1994)
- 26 F. Keilmann, R. Hillenbrand, *Philos. Trans. R. Soc. London A* **362**, 787 (2004)
- 27 D. Lide, *CRC Handbook of Chemistry and Physics* (CRC Press, 1990–91)
- 28 M. Thomas, J.-J. Greffet, R. Carminati, J.R. Arias-Gonzalez, *Appl. Phys. Lett.* **85**, 3863 (2004)
- 29 L. Novotny, *Appl. Phys. Lett.* **69**, 3806 (1996)
- 30 H. Gersen, M.F. Garcia-Parajo, L. Novotny, J.A. Veerman, L. Kuipers, N.F. van Hulst, *Phys. Rev. Lett.* **85**, 5312 (2000)
- 31 M. Böhmer, J. Enderlein, *J. Opt. Soc. Am. B* **20**, 554 (2003)
- 32 W. Stutzman, G. Thiele, *Antenna Theory and Design* (Wiley, New York, 1981)